

Supplement for: The Diet of Early Birds Based on Modern and Fossil Evidence and a New Framework for its Reconstruction

Supplemental Figures

Each of the figures herein are comparisons between key graphs from the literature [redrawn] and revised versions produced using reanalysed data. The figures mimic the aesthetics of the original graphs to make comparisons easier. Specifics are described in each figure caption.

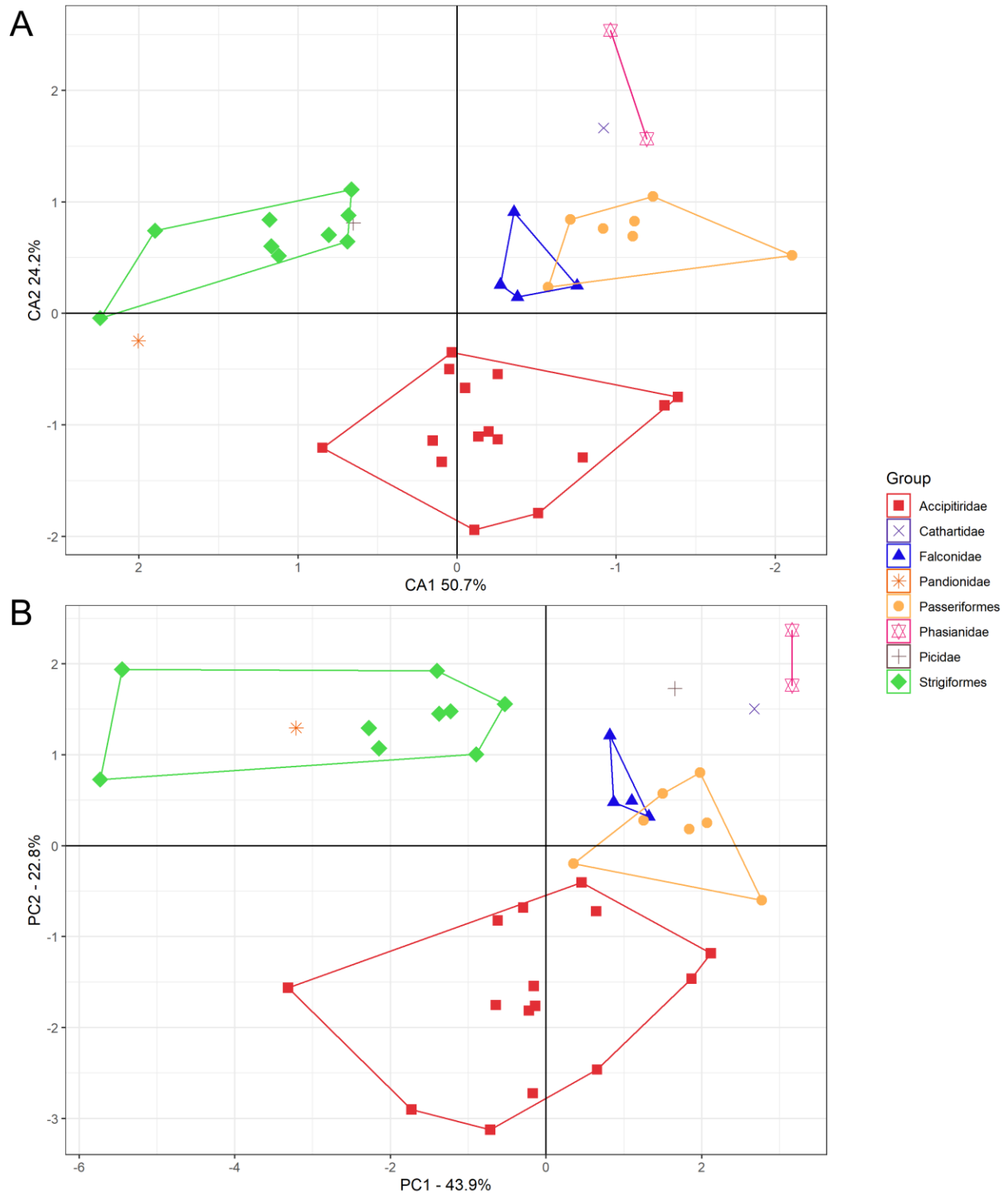


Fig. S1.

Principal Component Analysis [PCA] of avian pedal measurements. Fowler *et al.* (2009; 2011) use Correspondence Analysis [CA], designed to analyse discrete data, to analyse the continuous length measurements of the avian pes. (A) The original CA of Fowler *et al.* (2011) is provided, excluding

samples of *Deinonychus*. It generally resembles that of Fowler et al (2009) but has several additional strigiform samples included. This is contrasted to (B) PCA of the data used in (Fowler *et al.*, 2011) excluding *Deinonychus*. Note relative occupations of the morphospace by each group remains somewhat constant, but several differences are pertinent between the CA and PCA plots. In PCA: Pandionidae inhabits the same region of the morphospace as Strigiformes; Phasianidae, Piciformes, and Cathartidae cluster more closely to each other than any other groups; and in the set of Accipitridae, Falconidae, and Passeriformes, Passeriformes replaces Falconidae as the intermediary region and all three cluster more closely together.

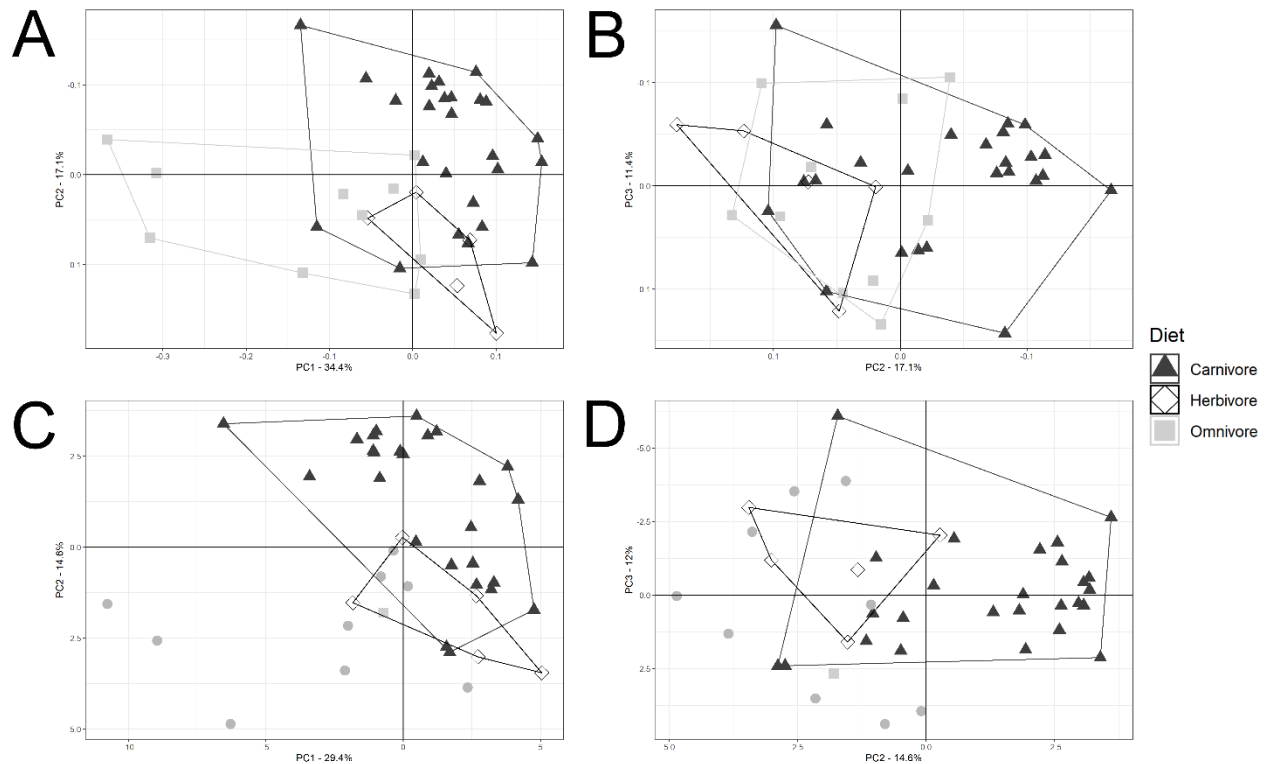


Fig. S2.

Principal Component Analysis of theropod skulls. The analysis of (A,B) Foth and Rauhut (2013) [convex hulls added] defines nine taxa as carnivorous, herbivorous, or omnivorous that this study considers indeterminate. In addition, their study does not scale the variance of the inputs when computing principal components. (C,D) Reanalysis with these taxa labelled as indeterminate and input variances scaled maintains most carnivores in their own region of the morphospace and lessens the overlap between carnivore and herbivore taxa (though the extreme morphologies of *Anchiornis* and *Bambiraptor* cause the convex hulls of the two to overlap broadly). No hull is generated for omnivores as the only taxon included with convincing evidence of omnivory is *Lesothosaurus* (Sciscio, Knoll, Bordy *et al.*, 2017). Note that the Y-axis of (A,C) and both axes of (B,D) are inverted relative to the original publication as the sign of principal components calculated with the `prcomp` function in R is arbitrary (R Core Team 2019).

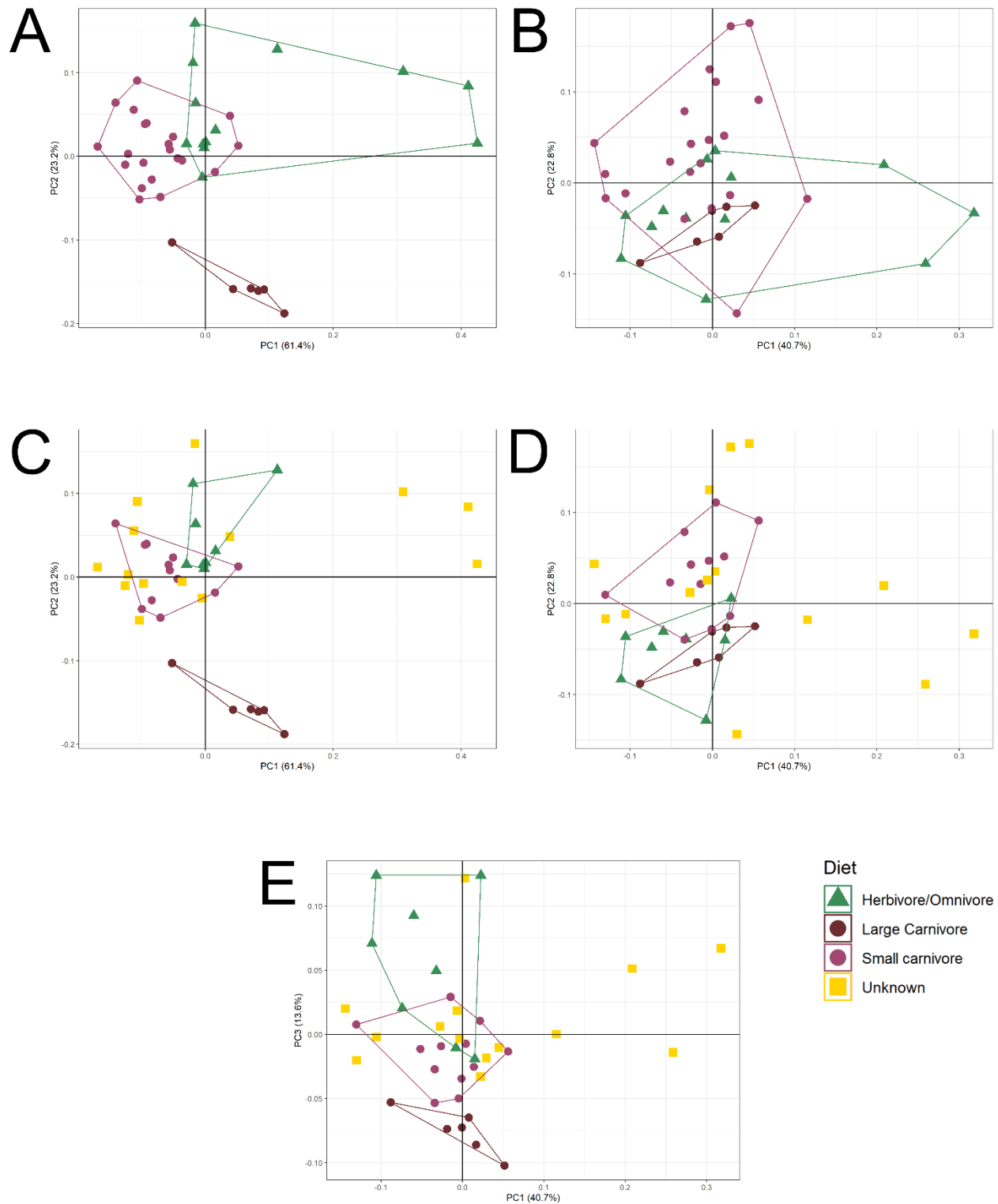


Fig. S3.

Principal Component Analysis of theropod skulls. (A,B) The analysis of Schaeffer *et al.* (2019) defines 14 taxa as herbivorous/omnivorous or as small carnivores that this study considers indeterminate. (C,D) Reanalysis with these taxa labelled as indeterminate decreases the overlap between herbivores/omnivores

and small carnivores primarily by removing therizinosaurians and avialans, respectively, from their groups. The total morphospace occupied by herbivores/omnivores is also greatly reduced by excluding oviraptorids which occupy their own unique area of the morphospace. PC1 and PC3 of landmark results are also plotted (E) to display their similarity to (A) and (C). This similarity is because PC3 of the landmark data describes similar shape variation to PC2 of the outline data (Figure 4 in Schaeffer *et al.*, 2019).

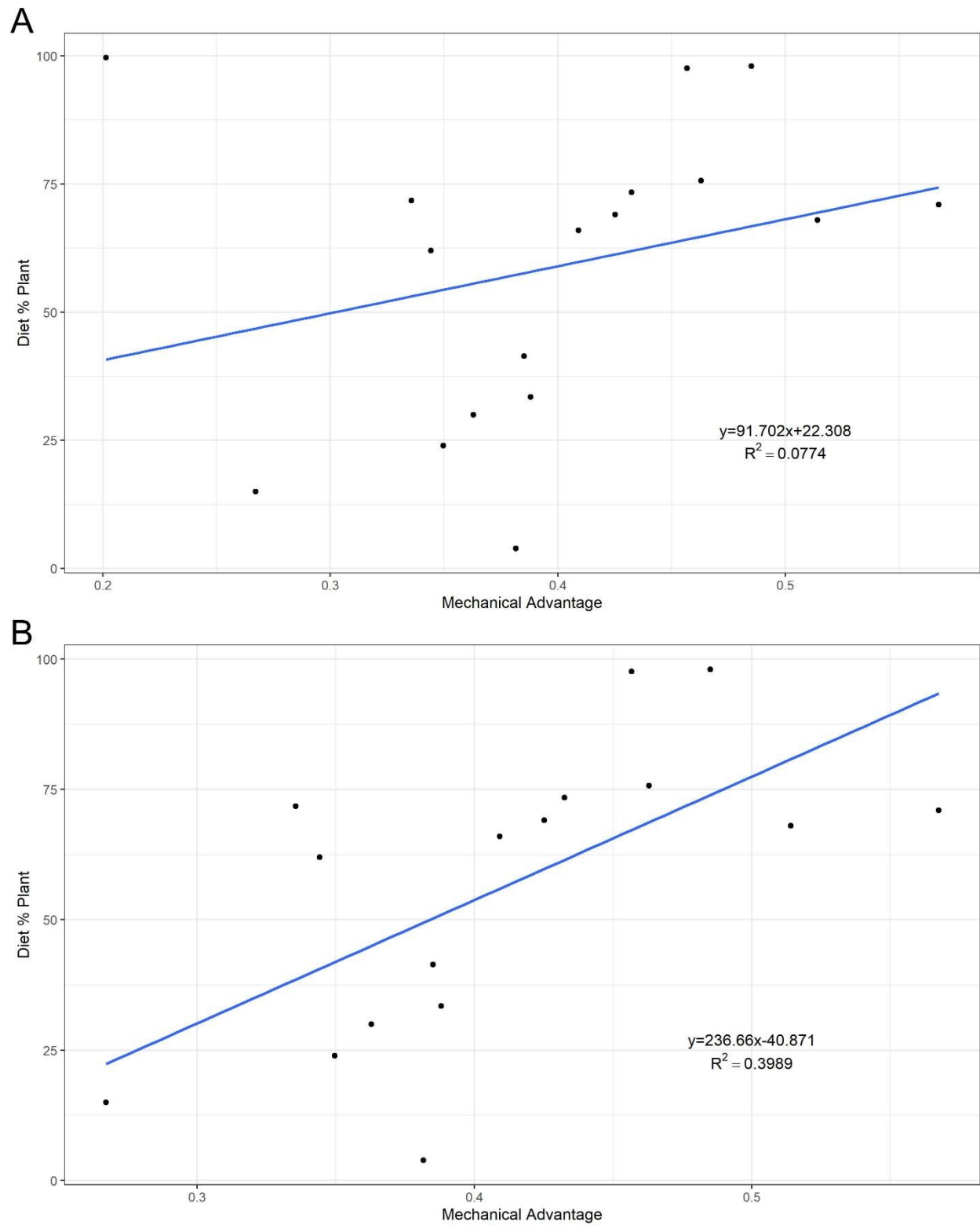


Fig. S4.

Relationship between mechanical advantage and plant consumption in Passerines. Plot based on the appendix of Corbin *et al.* (2015), (A) including and (B) excluding *Zenaida macroura*. *Z. macroura* is the

only columbiform bird included in the otherwise passerine data set. Correlation including this point included is weak to nonexistent, but of moderate strength when the data is restricted to passerine taxa.

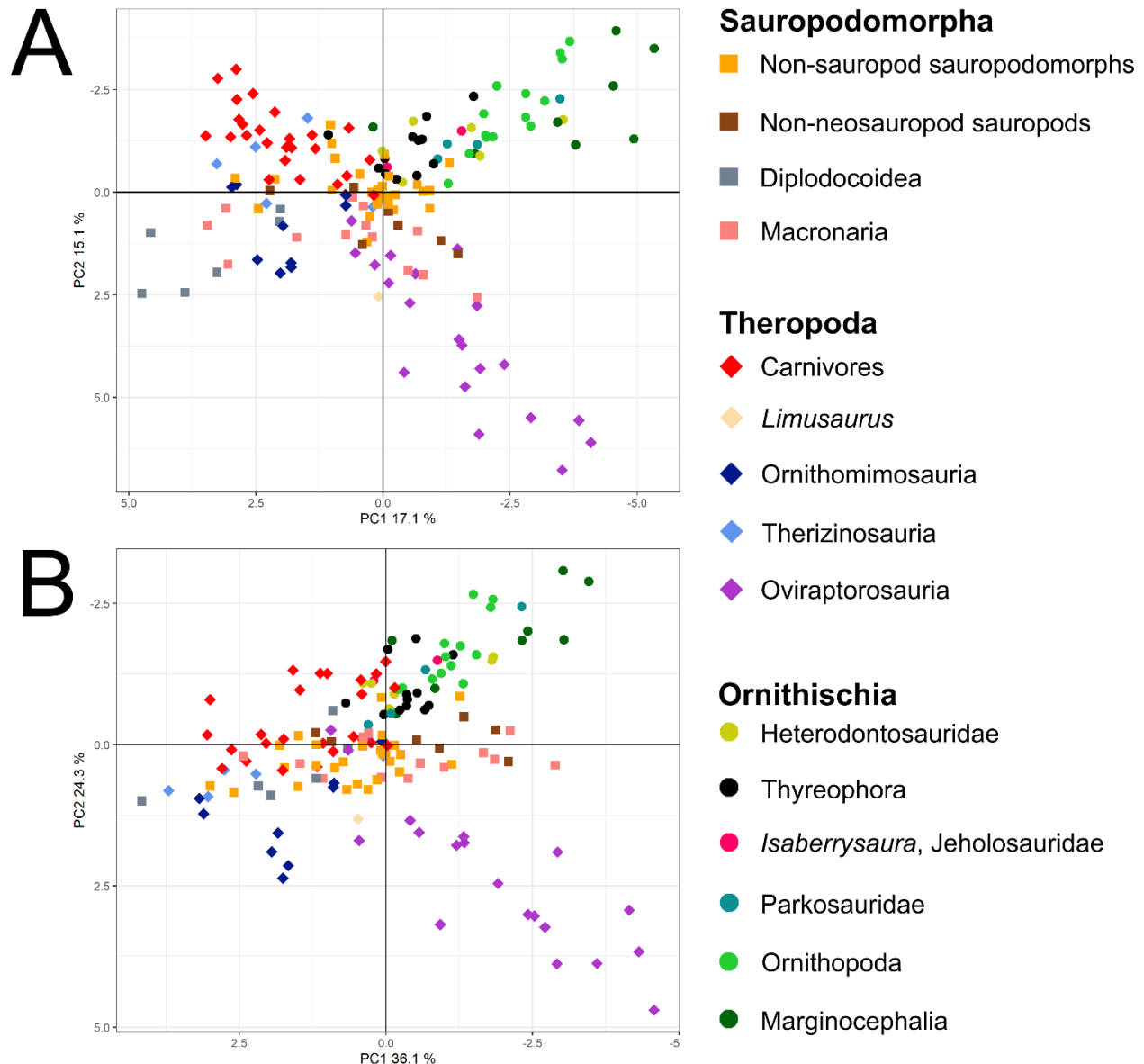


Fig. S5.

Biomechanical morphospace of Dinosauria. (A) The analysis of Button and Zanno (2020) incorporates 34 functional metrics to examine the affinities of various dinosaur groups in order to investigate convergence in dietary adaptation. Their observed trends are maintained in (B) an analysis incorporating only nine of their measured indices which have both theoretical validity and are shown to discriminate diet among extant animals [their C2–8, 22, and 23]. The most noteworthy difference in trends is that in (B) there is more separation in the morphospace between edentulous theropods [Ornithomimosauria and Oviraptorosauria] and sauropods along the PC2 axis. Note also that (B) accounts for a much higher proportion of the variance in the first two principal components [60.4% as opposed to 32.2% in (A)].

Both axes of the graphs are inverted relative to the original publication. An interactive three-dimensional graph of the data can be generated from the supplemental R code.

Supplemental Tables

The following are tables to assist in interpreting the details of this review. Specifics are given with each table caption.

Table S1.

Calculation of cranial connective properties of *Shenqiornis*. Connective tissue properties recorded in the literature are compiled and used to estimate connective tissue properties for *Shenqiornis*. Regressions of cross-sectional area [X-Sect] and Young's Modulus [E] were made vs. [body mass]^{0.33} using a polynomial [Poly] and power [Pow] fit to the properties of cranial sutures. As Cost *et al.* (2019) considered dog patellar tendon as a potential model, an additional power-fit regression using the full sample [PowFS] was also made. Macaques were excluded from all regressions as outliers. The properties of the Pow regression are used in Figure 6C; Poly and PowFS properties produced dislocation similar to Figure 6A and B.

Animal	Part	Mass (g)	X-Sect (mm ²)	E (MPa)	Source	Mass Source
Human Child	Cranial suture	27260.90	14.06	1100.00	(Davis, Loyd, Shen <i>et al.</i> , 2012)	(Davis <i>et al.</i> , 2012)
Human Infant	Cranial suture	10714.29		381.48	(Wang, Zou, Li <i>et al.</i> , 2014)	WHO weight-for-age 50th percentile at 18 months, weighted by gender
Human Postnatal	Cranial suture	8650.00		0.60	(Grau, Daw, Patel <i>et al.</i> , 2006)	WHO weight-for-age 50th percentile at 9 months
Macaque (male)	Cranial suture	5360.00		7700.00	(Kupczik, Dobson, Fagan <i>et al.</i> , 2007)	(Smith & Jungers, 1997)
Macaque (female)	Cranial suture	3590.00		1900.00	(Kupczik <i>et al.</i> , 2007)	(Smith <i>et al.</i> , 1997)
Mouse	Cranial suture	24.00	0.13	0.58	(Chien, Wu, Chao <i>et al.</i> , 2008)	(Chien <i>et al.</i> , 2008)
Lewis Rat	Cranial suture	250.50	0.51	2.35	(Chien <i>et al.</i> , 2008)	(Chien <i>et al.</i> , 2008)

Wistar Rat	Cranial suture	62.12		1.08	(McLaughlin, Zhang, Pashley <i>et al.</i> , 2000)	(Extrapolated from Novelli, Diniz, Galhardi <i>et al.</i> , 2007)
Rabbit	Facial suture	1590.57		1.27	(Radhakrishnan & Mao, 2004)	(Jones, Bielby, Cardillo <i>et al.</i> , 2009)
Goat	Nasal suture	46900.00		400.00	(Farke, 2008)	(Jones <i>et al.</i> , 2009)
Camel	Nuchal ligament	488000.00	850.00	0.55	(Dimery, Alexander & Deyst, 1985)	(Jones <i>et al.</i> , 2009)
Deer	Nuchal ligament	20000.00	51.60	0.61	(Dimery <i>et al.</i> , 1985)	(Dimery <i>et al.</i> , 1985)
Sheep	Nuchal ligament	21000.00	84.00	0.57	(Dimery <i>et al.</i> , 1985)	(Dimery <i>et al.</i> , 1985)
Pig	Palatal suture	84500.00	462.71	47.43	(Savoldi, Xu, Tsoi <i>et al.</i> , 2018)	(Jones <i>et al.</i> , 2009)
Dog	Patellar tendon	26700.00	0.24	30.80	(Haut, Lancaster & DeCamp, 1992)	(Haut <i>et al.</i> , 1992)
Reptile (validated in <i>Sphenodon</i> ?)	Suture	195.29		10.00	(Curtis, Jones, Evans <i>et al.</i> , 2013)	(Average of Herrel, Moore, Bredeweg <i>et al.</i> , 2010 Supplement 1)
<i>Shenqiornis</i> Poly		340.00	0.63	2.76	Regressions	Table 1, this review
<i>Shenqiornis</i> Pow		340.00	7.07	2.86	Regressions	Table 1, this review
<i>Shenqiornis</i> PowFS		340.00	0.68	2.51	Regressions	Table 1, this review

Supplemental References

- BUTTON D. J. & ZANNO, L. E. (2020). Repeated evolution of divergent modes of herbivory in non-avian dinosaurs. *Current Biology* **30**, 158-168. e4.
- CHIEN C. H., WU, Y. D., CHAO, Y.-J., CHEN, T., CHEN, W. F., YU, J. C. & LI, X. (2008). The effects of different cranial modules on mechanical properties of cranial suture in Lewis Rats and same-aged C57BL/6 Mice. *Strain* **44**, 272-277.
- CORBIN C. E., LOWENBERGER, L. K. & GRAY, B. L. (2015). Linkage and trade-off in trophic morphology and behavioural performance of birds. *Functional Ecology* **29**, 808-815.
- COST I. N., MIDDLETON, K. M., SELLERS, K. C., ECHOLS, M. S., WITMER, L. M., DAVIS, J. L. & HOLLIDAY, C. M. (2019). Palatal biomechanics and its significance for cranial kinesis in *Tyrannosaurus rex*. *The Anatomical Record: Advances in Integrative Anatomy and Evolutionary Biology*.
- CURTIS N., JONES, M. E. H., EVANS, S. E., O'HIGGINS, P. & FAGAN, M. J. (2013). Cranial sutures work collectively to distribute strain throughout the reptile skull. *Journal of the Royal Society Interface* **10**, 20130442.
- DAVIS M. T., LOYD, A. M., SHEN, H.-Y. H., MULROY, M. H., NIGHTINGALE, R. W., MYERS, B. S. & BASS, C. D. (2012). The mechanical and morphological properties of 6 year-old cranial bone. *Journal of Biomechanics* **45**, 2493-2498.
- DIMERY N. J., ALEXANDER, R. M. & DEYST, K. A. (1985). Mechanics of the ligamentum nuchae of some artiodactyls. *Journal of Zoology* **206**, 341-351.
- FARKE A. A. (2008). Frontal sinuses and head-butting in goats: a finite element analysis. *Journal of Experimental Biology* **211**, 3085-3094.
- FOTH C. & RAUHUT, O. W. M. (2013). Macroevolutionary and morphofunctional patterns in theropod skulls: a morphometric approach. *Acta Palaeontologica Polonica* **58**, 1-16.
- FOWLER D. W., FREEDMAN, E. A. & SCANNELLA, J. B. (2009). Predatory functional morphology in raptors: interdigital variation in talon size is related to prey restraint and immobilisation technique. *PLOS ONE* **4**, e7999.
- FOWLER D. W., FREEDMAN, E. A., SCANNELLA, J. B. & KAMBIC, R. E. (2011). The predatory ecology of *Deinonychus* and the origin of flapping in birds. *PLOS ONE* **6**, e28964.
- GRAU N., DAW, J. L., PATEL, R., EVANS, C., LEWIS, N. & MAO, J. J. (2006). Nanostructural and nanomechanical properties of synostosed postnatal human cranial sutures. *Journal of Craniofacial Surgery* **17**, 91-98.
- HAUT R. C., LANCASTER, R. L. & DECAMP, C. E. (1992). Mechanical properties of the canine patellar tendon: some correlations with age and the content of collagen. *Journal of Biomechanics* **25**, 163-173.
- HERREL A., MOORE, J. A., BREDEWEG, E. M. & NELSON, N. J. (2010). Sexual dimorphism, body size, bite force and male mating success in tuatara. *Biological Journal of the Linnean Society* **100**, 287-292.
- JONES K. E., BIELBY, J., CARDILLO, M., FRITZ, S. A., O'DELL, J., ORME, C. D. L., SAFI, K., SECHREST, W., BOAKES, E. H., CARBONE, C., CONNOLLY, C., CUTTS, M. J., FOSTER, J. K., GRENYER, R., HABIB, M., PLASTER, C. A., PRICE, S. A., RIGBY, E. A., RIST, J., TEACHER, A.,

- BININDA-EMONDS, O. R. P., GITTLEMAN, J. L., MACE, G. M. & PURVIS, A. (2009). PanTHERIA: a species-level database of life history, ecology, and geography of extant and recently extinct mammals. *Ecology* **90**, 2648-2648.
- KUPCZIK K., DOBSON, C. A., FAGAN, M. J., CROMPTON, R. H., OXNARD, C. E. & O'HIGGINS, P. (2007). Assessing mechanical function of the zygomatic region in macaques: validation and sensitivity testing of finite element models. *Journal of Anatomy* **210**, 41-53.
- MCLAUGHLIN E., ZHANG, Y. G., PASHLEY, D., BORKE, J. & YU, J. C. (2000). The load-displacement characteristics of neonatal rat cranial sutures. *The Cleft Palate-Craniofacial Journal* **37**, 590-595.
- NOVELLI E. L. B., DINIZ, Y. S., GALHARDI, C. M., EBAID, G. M. X., RODRIGUES, H. G., MANI, F., FERNANDES, A. A. H., CICOGNA, A. C. & NOVELLI FILHO, J. L. V. B. (2007). Anthropometrical parameters and markers of obesity in rats. *Laboratory animals* **41**, 111-119.
- R CORE TEAM. (2019). prcomp function | R Documentation Version 3.6.2.
- RADHAKRISHNAN P. & MAO, J. J. (2004). Nanomechanical properties of facial sutures and sutural mineralization front. *Journal of dental research* **83**, 470-475.
- SAVOLDI F., XU, B., TSOI, J. K. H., PAGANELLI, C. & MATINLINNA, J. P. (2018). Anatomical and mechanical properties of swine midpalatal suture in the premaxillary, maxillary, and palatine region. *Scientific Reports* **8**, 1-12.
- SCHAEFFER J., BENTON, M. J., RAYFIELD, E. J. & STUBBS, T. L. (2019). Morphological disparity in theropod jaws: comparing discrete characters and geometric morphometrics. *Palaeontology* **63**, 283-299.
- SCISCIO L., KNOLL, F., BORDY, E. M., DE KOCK, M. O. & REDELSTORFF, R. (2017). Digital reconstruction of the mandible of an adult *Lesothosaurus diagnosticus* with insight into the tooth replacement process and diet. *PeerJ* **5**, e3054.
- SMITH R. J. & JUNGERS, W. L. (1997). Body mass in comparative primatology. *Journal of Human Evolution* **32**, 523-559.
- WANG J., ZOU, D., LI, Z., HUANG, P., LI, D., SHAO, Y., WANG, H. & CHEN, Y. (2014). Mechanical properties of cranial bones and sutures in 1–2-year-old infants. *Medical Science Monitor: International Medical Journal of Experimental and Clinical Research* **20**, 1808.